The Design of a Pulse Generator for a Diffraction Field Computer

A Thesis

Submitted by

Sidney A. Radley

(April, 1950)

In partial fulfilment of the requirements of the Faculty of Graduate Studies and Research at McGill University for the degree of Master of Science.

Contents

Contents - cont'd

Index to Illustrations and Tables

ACKNOWLEDGEMENTS

To Professor G.A. Woonton for his constant supervision and encouragement in this research, I tender sincere appreciation and thanks.

My deepest gratitude also to Mr. C.H.M. Turner for his interest and invaluable suggestions.

Dr. H.G.I. Watson kindly made available equipment necessary for the research.

A National Research Council Bursary enabled the author to devote full time to this research for one year.

Symbols

φ: Intensity of radiation

r: Linear distance from radiator to point of observation

c: Velocity of propogation

λ: Wavelength in centimeters

t: Time in seconds

cm.: Centimeters

μsec.: Microseconds

Mc/sec.: Megacycles per second

Kc/sec.: Kilocycles per second

C.P.S.: Cycles per second

P.R.F.: Pulse Recurrence Frequency

Abstract

A computer may be defined as a device that performs mathematical operations on input data to yield results which may otherwise be obtained by more laborious and time-consuming methods. Analogue computers represent a general method of using one physical system as a model for another system, more difficult to construct or measure, that obeys equations of the same form. An analogue computer is one which deals with continuously variable physical magnitude; a simple example is the use of an electrolytic trough to plot lines of current flow between immersed electrodes, which are analogous to the lines of electric intensity between similar electrodes in free space. This paper deals with the analogy between the distant field of a radiating linear antenna, and the frequency spectrum of a voltage pulse. The mathematical analogy is first developed, from which the specifications on the pulse are obtained. The major part of the paper deals with the design of electronic circuits to produce the desired pulse. Its frequency spectrum has been examined, and photographs obtained to illustrate the computer representation of the field intensity from certain types of microwave horn radiators.

The Design of a Pulse Generator for a Diffraction Field Computer

Sidney A. Radley

(April, 1950)

Summary

The experimental solution of some problems in physics is laborious and time-consuming. Analogue computers represent a general method of using one physical system as a model for another system, more difficult to construct or measure, that obeys equations of the same form. This paper deals with the analogy between the distant field of a radiating linear antenna, and the frequency spectrum of a voltage pulse. The mathematical analogy is first developed, from which the specifications of the pulse are obtained. The major part of the paper deals with the design of electronic circuits to produce the desired pulse. Its frequency spectrum has been examined, and photographs obtained to illustrate the computer representation of the field intensity from certain types of microwave horn radiators.

Macdonald Physics Building M.Sc.

1. The Physical and Mathematical Analysis of the Diffraction Field

1: 1. Theoretical Introduction

A natural consequence of the increased use of shorter wavelengths in radio is the application of the methods of physical optics to the calculation of intensity distribution of electromagnetic radiation from radiating systems. The relation from which most optical diffraction formulae can be derived is given by Slater and Frank as (1)

$$\Phi = -\frac{1}{4\pi}\int_V \frac{\left[\nabla^2\Phi - \frac{1}{c^2}\frac{\partial^2\Phi}{\partial t^2}\right]}{r}\,dV + \frac{1}{4\pi}\int_S \frac{1}{r}\left\{\left[\frac{1}{c}\frac{\partial\Phi}{\partial t} + \frac{\Phi(t-\frac{r}{c})}{r}\right]\cos(nr) + \frac{\partial\Phi}{\partial n}\right\}da \qquad (1)$$

where Φ = intensity of radiation

r = distance from radiator to point of observation

c = velocity of wave propogation

nr = angle between the normal to the radiator and the vector r

Experiments have shown that this equation can be made to predict radio fields with good accuracy.

It is convenient for calculations to imagine that the antenna aperture is a hole cut symmetrically about the origin of axes, in an infinite shield that lies in the (x,y) plane; the surface of integration must be completed by an infinite hemisphere, also a shield, which has its base on the (x,y) plane and encloses the point of observation P(x',y',z').

The equation which corresponds to the derivation from equation (1) by Slater and Frank is [2]

$$\varphi(x';y';z') = \frac{1}{4\pi}\int_s \frac{f(x,y)}{r} e^{j\omega(t-\frac{r}{c})}\left[\left(\frac{1}{r}+j\frac{\omega}{c}\right)\cos(nr)+j\frac{\omega}{c}\right]da \qquad (2)$$

The integration is over the aperture only, as the sole contributor to the field. Two further approximations are generally made, which are justified by experimental results:

(1) $r >> \lambda$ so that $\left(\frac{1}{r}+j\frac{\omega}{c}\right) = \frac{1}{r}+j\frac{2\pi}{\lambda} \doteq j\frac{2\pi}{\lambda}$

(11) (nr) is a small angle (less than 35 or 40 degrees) so that (1 + cos nr) is almost constant and may be taken from under the integration sign.

Then equation (2) becomes

$$\varphi(x';y';z') = \frac{j}{2\lambda}(1+\cos(nr))\, e^{j\omega t}\int_A \frac{f(x,y)}{r} e^{-j\frac{2\pi}{\lambda}r}\, da \qquad (3)$$

The field across the mouth of an electromagnetic horn can be written in the form f(x,y) = F(x)F(y), so that the integral containing f(x,y) in equation (3) may be broken into the product of two integrals:

$$\varphi(x';y';z') = (1+\cos(nr))\, e^{j\omega t}\sqrt{\frac{j}{2\lambda}}\int_a \frac{F(y)}{\sqrt{r}}\cdot\sqrt{\frac{j}{2\lambda}}\int_A \frac{F(x)}{r} e^{-j\frac{2\pi}{\lambda}r}\, dy\, dx \qquad (4)$$

When the point (x',y',z') is at a distance from the aperture great compared to aperture width and wavelength, r becomes a constant R with respect to the

amplitude contributions from each aperture element. However, the phase contribution from each element of aperture must be taken into consideration. Usually only variations in the distant field with changes in x' (or y') are observed. If only variations with x' are observed, the integral containing F(y) in (4) becomes a constant Y. Let the aperture lie in the (x,y) plane as in Fig. 1, with the aperture centre at the origin of axes (x,y,z).

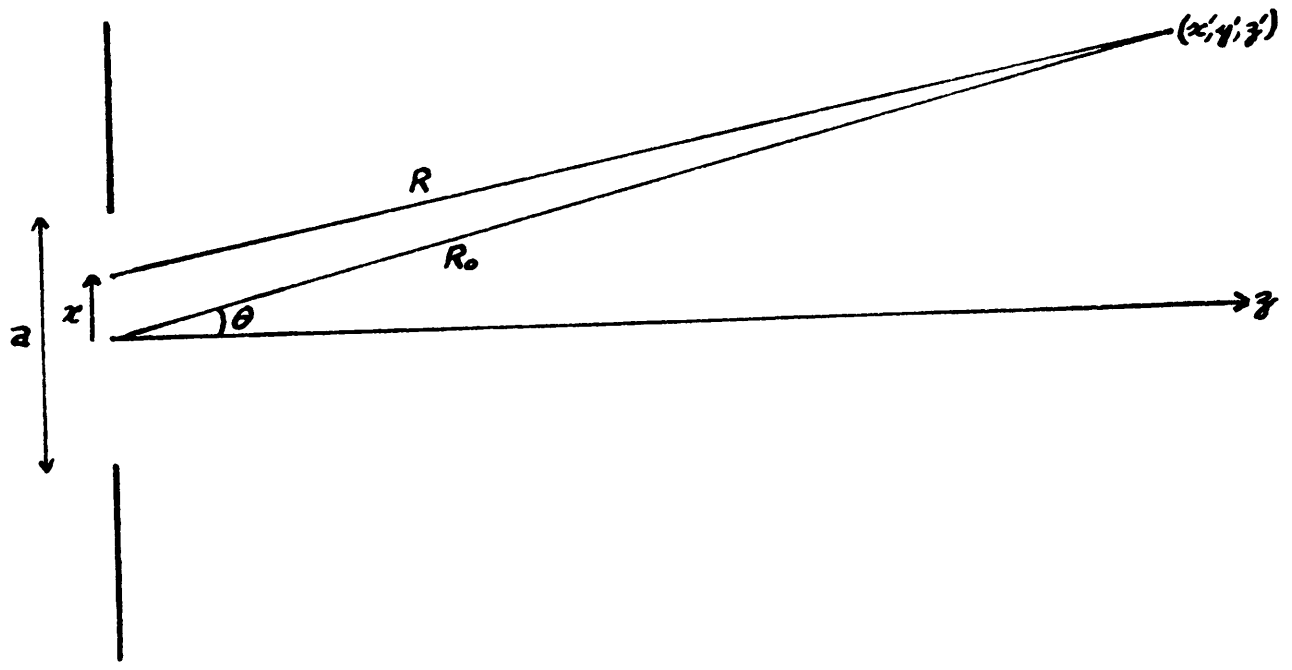

Fig. 1

$$R = (R_0^2 + x^2 - 2R_0 x \sin\theta)^{1/2} \qquad \because \; R_0^2 \gg x^2$$

$$\therefore R = R_0 - x\sin\theta + O\left(\frac{x\sin\theta}{R_0}\right)$$

$$\doteq R_0 - x\sin\theta$$

Then equation (4) may be written

$$\varphi\left(\frac{\sin\theta}{\lambda}\right) = \left(1+\cos(n\pi)\right) e^{j\omega t} \gamma \sqrt{\frac{j}{2\lambda R}} \int_{-\frac{a}{2}}^{a/2} F(x)\, e^{-j\frac{2\pi}{\lambda}(R_0 - x\sin\theta)}\, dx$$

$$= \left(1+\cos(n\pi)\right) e^{j\omega\left(t-\frac{R_0}{c}\right)} \gamma \sqrt{\frac{j}{2\lambda R}} \int_{-\frac{a}{2}}^{a/2} F(x)\, e^{j2\pi x\frac{\sin\theta}{\lambda}}\, dx \qquad (5)$$

1: 2. The Fourier Integral Representation of the Distant Field.

The function F(x) which represents the x-distribution of intensity in the aperture of a linear radiator is of that class that can be represented by a Fourier Integral:

$$F(x) = \frac{1}{2\pi} \iint_{-\infty}^{\infty} F(\xi)\cos\gamma(\xi - x)\, d\xi\, d\gamma \qquad (6)$$

or in its equivalent exponential form

$$F(x) = \iint_{-\infty}^{\infty} F(\xi)\, e^{j2\pi\gamma(x-\xi)}\, d\xi\, d\gamma$$

$$= \int_{-\infty}^{\infty} \left[\int_{-\infty}^{\infty} F(\xi)\, e^{-j2\pi\gamma\xi}\, d\xi \right] e^{j2\pi\gamma x}\, d\gamma \qquad (7)$$

If the bracketed integral of (7) is defined by $G(\gamma)$, then there appears a pair of integrals which transform $G(\gamma)$ into F(x) and F(x) into $G(\gamma)$:

$$G(\gamma) = \int_{-\infty}^{\infty} F(\xi)\, e^{-j2\pi\gamma\xi}\, d\xi \qquad (8)$$

$$F(x) = \int_{-\infty}^{\infty} G(\gamma) e^{j2\pi\gamma x} d\gamma \qquad (9)$$

Compare (8) and (9) with (5). The limits of integration of (5) could be from $-\infty$ to ∞ without altering its value, as the sole contributor to the field is the aperture of width "a". If "γ" is defined to be $-\frac{\sin\theta}{\lambda}$, then $G(\gamma)$ is an integral that gives the variable part of the distant field from a linear radiator. From (9), if the distant field is known, the aperture distribution can be found.

1: 3. The Fourier Integral Representation of an Electrical Pulse.

A pulse of voltage which exists only for a time T, and is zero at all other times can also be represented by a Fourier Integral:

$$F(t) = \int_{-\infty}^{\infty}\int_{-\infty}^{\infty} F(\xi) e^{j2\pi f(t-\xi)} d\xi\, df$$

$$= \int_{-\infty}^{\infty}\left[\int_{-\infty}^{\infty} F(\xi) e^{-j2\pi f\xi} d\xi\right] e^{j2\pi ft} df \qquad (10)$$

If the bracketed integral of (11) is defined by G(f), then there appears a pair of integrals which transform G(f) into F(t) and F(t) into G(f):

$$G(f) = \int_{-\infty}^{\infty} F(\xi) e^{-j2\pi f\xi} d\xi \qquad (11)$$

$$F(t)=\int_{-\infty}^{\infty} G(f)\,e^{j2\pi ft}\,df \qquad (12)$$

Equation (11) implies that corresponding to the time representation of the pulse, F(t), there exists a frequency spectrum G(f) which can be found by performing the integration; or if the frequency spectrum G(f) is given, the time representation can be found from (12).

1:4. Pulse Analogue of the Distant Field

Because equations (8) and (11), (9) and (12) correspond in form it is possible to calculate the distant pattern $G(\gamma)$ of an antenna from its aperture distribution F(x) by setting up a pulse analogue F(t) and investigating its frequency spectrum G(f). A convenient and direct representation of the result would be to display the frequency spectrum of the pulse on a cathode ray tube.

In order to establish the correspondence between the variables in the two cases, compare the distant field of an aperture "a" wide in which the field distribution is $F(x)e^{jwt}$, $(x)\leq\frac{a}{2}$, with the frequency spectrum of a pulse whose voltage is given by

$$F(t)e^{j2\pi f_c t} \qquad ,|t|\leq\frac{T}{2}$$

Then

$$G\left(-\frac{\sin\theta}{\lambda}\right)=e^{j\omega t}\int_{-\frac{a}{2}}^{a/2} F(x)\,e^{j2\pi x\frac{\sin\theta}{\lambda}}\,dx \qquad (13)$$

and

$$G(f_o-f)=\int_{-T/2}^{T/2}F(t)e^{j2\pi(f_o-f)t}\,dt \tag{14}$$

Equation (13) is obtained from (8), and (14) from (11).

Now let F(x) = A and substitute in (13):

$$G\left(-\frac{\sin\theta}{\lambda}\right)=Ae^{j\omega t}\int_{-a/2}^{a/2}e^{j2\pi x\frac{\sin\theta}{\lambda}}\,dx$$

$$=Ae^{j\omega t}\left[\frac{\sin\left(\pi a\frac{\sin\theta}{\lambda}\right)}{}\right.$$

$$=Aa\,e^{j\omega t}\,\frac{\sin\left(\pi a\frac{\sin\theta}{\lambda}\right)}{\pi a\frac{\sin\theta}{\lambda}} \tag{13a}$$

Let F(t) = B and substitute in (14):

$$G(f_o-f)=B\int_{-T/2}^{T/2}e^{j2\pi(f_o-f)t}\,dt$$

$$=BT\,\frac{\sin[\pi T(f_o-f)]}{\pi T(f_o-f)} \tag{14a}$$

At corresponding points in the two patterns, relative amplitudes are the same:

$$\frac{\sin\left(\pi a\frac{\sin\theta}{\lambda}\right)}{\pi a\frac{\sin\theta}{\lambda}}=\frac{\sin[\pi T(f_o-f)]}{\pi T(f_o-f)}$$

$$\therefore\ a\frac{\sin\theta}{\lambda}=T(f_o-f) \tag{15}$$

From equations (13) and (14), the analogue of ($\frac{\sin\theta}{\lambda}$) is ($f_o - f$), and of "x" is "t". If the form of $G(f_o - f)$ is to be the same as that of $G(-\frac{\sin\theta}{\lambda})$, the form of F(t) must be the same as that of F(x). Equation (15) establishes the correspondence between the variables of the two systems.

2. Design Considerations

2: 1. Phase Relations in a Horn Aperture

Experiment has shown[5] that an electromagnetic horn may be treated as an aperture illuminated by a point source at the apex of the horn. Fig. 2 is a pictorial representation of a cross-section of a horn.

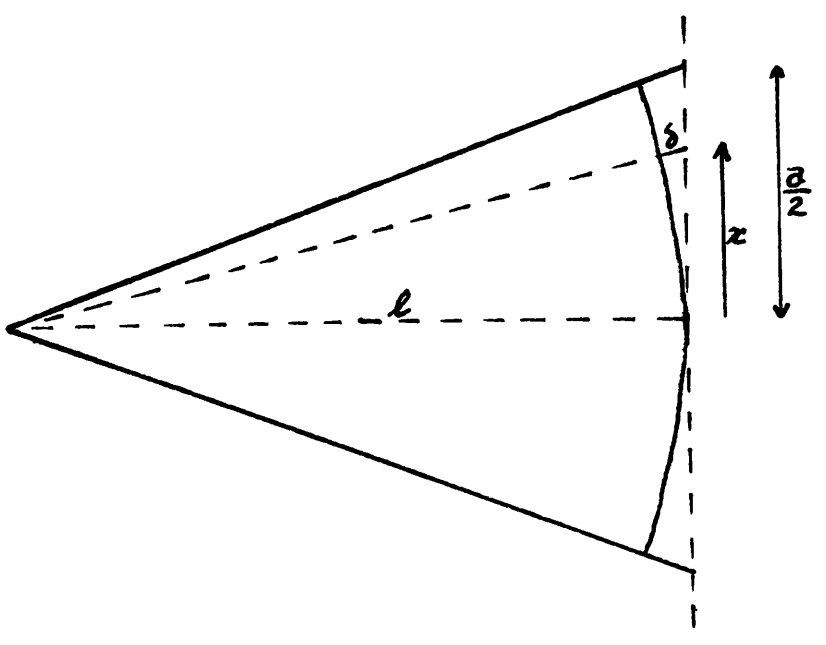

Fig. 2

The wavefront advancing down the horn is not plane, so there will be variations in phase across the horn. The amount of phase change a distance "x" from the

centre of the mouth of the horn will depend on the curvature of the wavefront, that is on the length δ in Fig. 2:

$$x^2+\ell^2=(\ell+\delta)^2=\ell^2+2\ell\delta+\delta^2$$

$$\therefore \delta=-\ell+\sqrt{\ell^2+x^2} \qquad :: \qquad \{\delta=0 \text{ at } x=0\}$$

$$=-\ell+\ell\left(1+\frac{x^2}{\ell^2}\right)^{1/2}$$

$$=-\ell+\ell\left[1+\frac{x^2}{2\ell^2}-\frac{x^4}{8\ell^4}+\frac{3x^6}{48\ell^6}-\ldots.\right]$$

$$=\frac{x^2}{2\ell}-\frac{x^4}{8\ell^3}+\frac{3x^6}{48\ell^5}-\ldots\ldots$$

The physical dimensions of horns which are most often used show that less than 1.5% error in δ is introduced by neglecting all terms beyond the first, so that to a very good approximation

$$\delta(x)=\frac{x^2}{2\ell} \tag{16}$$

If the coordinate system is chosen so that the E - vector in the aperture is in the y direction, then the field in the E-plane can be described by

$$F(x)=A\,e^{j\left(\omega t-\frac{2\pi}{\lambda}\delta(x)\right)} \qquad , |x|\leq\frac{a}{2} \tag{17}$$

where "a" is aperture width, and $\delta(x)$ is given by (16).

2: 2. Analogous Phase Relations in a Voltage Pulse.

Suppose that a pulse is obtained by gating the output of an oscillator, which is frequency modulated.

Such a pulse could have the form

$$F(t) = A e^{j(2\pi f_0 t - k\delta(t))} \tag{18}$$

where the phase change across the pulse, k δ(t), corresponds to the phase change across the aperture, $\frac{2\pi}{\lambda}\delta(x)$. For frequency modulation:

$$2\pi f = 2\pi f_0 - k\,Q(t) \qquad :: \quad \{k = 2\pi\Delta f\}$$

The phase ψ_1 of the oscillations is

$$\psi_1 = \int 2\pi f\,dt = 2\pi f_0 t - k\int Q(t)\,dt = 2\pi f_0 t - k\,\delta(t).$$

$$\therefore \delta(t) = \int Q(t)\,dt \tag{19}$$

Now consider equation (17), and let the phase be ψ_2:

$$\psi_2 = \omega t - \frac{2\pi}{\lambda}\delta(x) = \omega t - \frac{2\pi}{\lambda}\frac{x^2}{2\ell}$$

Let $\delta(x) = \frac{x^2}{2\ell} = \int P(x)\,dx$

Then $P(x) = \frac{x}{\ell}$ (20)

Therefore the function Q(t) of (19) must be of the form t/b to correspond to (20), and "b" has dimensions of time. The modulating waveform must then be linear in form for the phase change across the pulse to be parabolic. For correspondence

$$\frac{2\pi}{\lambda}\frac{x^2}{2\ell} = \frac{kt^2}{2b} \tag{20a}$$

2: 3. Design Criteria for Pulse Generating Circuits

The design of the computer was approached with the requirements that it should simulate measurements for which $0 \leq \frac{a}{\lambda} \leq 50$ and $-45^\circ \leq \theta \leq 45^\circ$, and be capable of discriminating relative amplitude down to 1°. Equation (15) can be used to interpret these data in terms of pulse length. Since sin 45° = 0.707, the whole frequency range must be

$$2(f_o - f) = 0.707 \times \frac{2a}{\lambda} \qquad (21)$$

To establish the correspondence for a 1° plotting accuracy notice that the change in sin θ is least at the greatest angles, and hence:

$$\text{at } 45^\circ, (f_o - f) = 0.707 \times \frac{a}{T\lambda}$$
$$\text{at } 46^\circ, (f_o - f) = 0.719 \times \frac{a}{T\lambda}$$
$$\therefore f(46^\circ) - f(45^\circ) = 0.012 \times \frac{a}{T\lambda} \qquad (22)$$

The spectrum analyzer must be capable of examining a frequency range $2(f_o - f)$ of the frequency spectrum of the pulse, which together with the required limits of values of a/λ limits the pulse length T to a certain time range. Substituting some of these values of T into equation (22) gives values of frequency bandwidth necessary in the analyzer receiver for the desired plotting accuracy.

A compromise between the two factors frequency range and frequency bandwidth led to a choice of 50 micro-seconds for the pulse width T. Substituting $a/\lambda = 50$ in equation (21) then gives the maximum frequency range to be examined as 1.4 Mc/sec.. As $2(f_o - f)$ must be a sufficiently small fraction of f_o to permit the range to be covered without amplitude modulation, f_o should be chosen as high as possible consistent with the use of conventional circuit components. A value for f_o was arbitrarily set at 30 Mc/sec..

The frequency sweep of the cathode ray tube presentation must simulate a plot of radiation intensity over a total angle of 90°, so there should be 90 display pulses on the tube. A long-persistence tube will perform satisfactorily with a sweep recurrence frequency of 10 c.p.s.. Hence the P.R.F. of the pulses from the pulse generating unit was chosen as 900 per second.

The two horns with the greatest phase change in present use at McGill are ones with $\ell = 100$ cms., $a = 64$ cms., for which

$$\frac{2\pi}{\lambda}\left(\frac{a}{2}\right)^2\frac{1}{2\ell} = 3\cdot 2\pi \qquad (23a)$$

and $\ell = 50$ cms., $a = 32$ cms., for which

$$\frac{2\pi}{\lambda}\left(\frac{a}{2}\right)^2\frac{1}{2\ell} = 1\cdot 6\pi \qquad (23b)$$

For T = 50 μsec. and f_o = 30 Kc/sec., a phase change of 3.2π in 25 μsec. means a frequency shift of 1.6 cycles in 750 cycles. (30 Kc/sec. is 750 cycles in 25 μsec.). Hence the frequency deviation is 64 Kc/sec.. Similarly for a phase change of 1.6π , the frequency deviation is 32 Kc/sec.. Using these values in equation (21) and solving for the constant "b" gives

$$b = \frac{kT^2\lambda\ell}{2\pi a^2} = 12.5\,\mu sec. \qquad (24)$$

This value of "b" checks if used in (21) for other corresponding values of "x" and "t" and "k".

The value of "k" in terms of the horn dimensions and transmitted wavelength may now be obtained:

$$k = \frac{2\pi}{\lambda}\left(\frac{a}{2}\right)^2\left(\frac{2}{T}\right)^2\frac{b}{\ell}\,sec^{-1} = \frac{\pi a^2}{\lambda\ell}\times 10^4\,sec^{-1} \qquad (25)$$

Therefore the frequency deviation Δf is given by

$$\Delta f = \frac{k}{2\pi} = \frac{5a^2}{\lambda\ell}\,kc/sec. \qquad (26)$$

In brief then, equation (26) gives the frequency deviation necessary to produce a phase change across the pulse corresponding to the phase change across the mouth of a rectangular horn, the dimensions of which are "a" and "ℓ", the transmitted frequency being of wavelength "λ".

For convenience, the analogous equations and variables are summarized here in Table 1.

Table 1.

Summary of Formulae, Analogies and Design Criteria

Eqn.	Radiating System	Eqn.	Computor
(8)	$G(\gamma)=\int_{-\infty}^{\infty}F(\xi)\,e^{-j2\pi\gamma\xi}\,d\xi$	(11)	$G(f)=\int_{-\infty}^{\infty}F(g)\,e^{-j2\pi fg}\,dg$
(9)	$F(x)=\int_{-\infty}^{\infty}G(\gamma)\,e^{j2\pi\gamma x}\,d\gamma$	(12)	$F(t)=\int_{-\infty}^{\infty}G(f)\,e^{j2\pi ft}\,df$
(13)	$G(-\frac{\sin\theta}{\lambda})=e^{j\omega t}\int_{-\frac{a}{2}}^{a/2}F(x)\,e^{j2\pi x\frac{\sin\theta}{\lambda}}\,dx$	(14)	$G(f_o-f)=\int_{-\frac{T}{2}}^{T/2}F(t)e^{j2\pi(f_o-f)t}\,dt$
(15)	$a\frac{\sin\theta}{\lambda}$	(15)	$T(f_o-f)$
	x		t
	$\frac{\sin\theta}{\lambda}$		(f_o-f)
(17)	$F(x)=Ae^{j[\omega t-\frac{2\pi}{\lambda}\delta(x)]}$	(18)	$F(t)=Ae^{j[2\pi f_o t-k\delta(t)]}$
	$\delta(x)=\frac{x^2}{2l}$		$\delta(t)=\frac{t^2}{2b}$
	3.2π (Max. Phase Shift)		64 kc/sec. (Freq. Deviation)
	$5\leq\frac{a}{\lambda}\leq 50$		$T=50\mu$sec
	$-45^\circ\leq\theta\leq 45^\circ$		$f_o=30$ Mc/sec.
			P.R.F. = 900 c.p.s.

3. Practical Considerations

3: 1. Block Diagram

Fig. 3 is a block diagram of the complete electronic analogue computor.

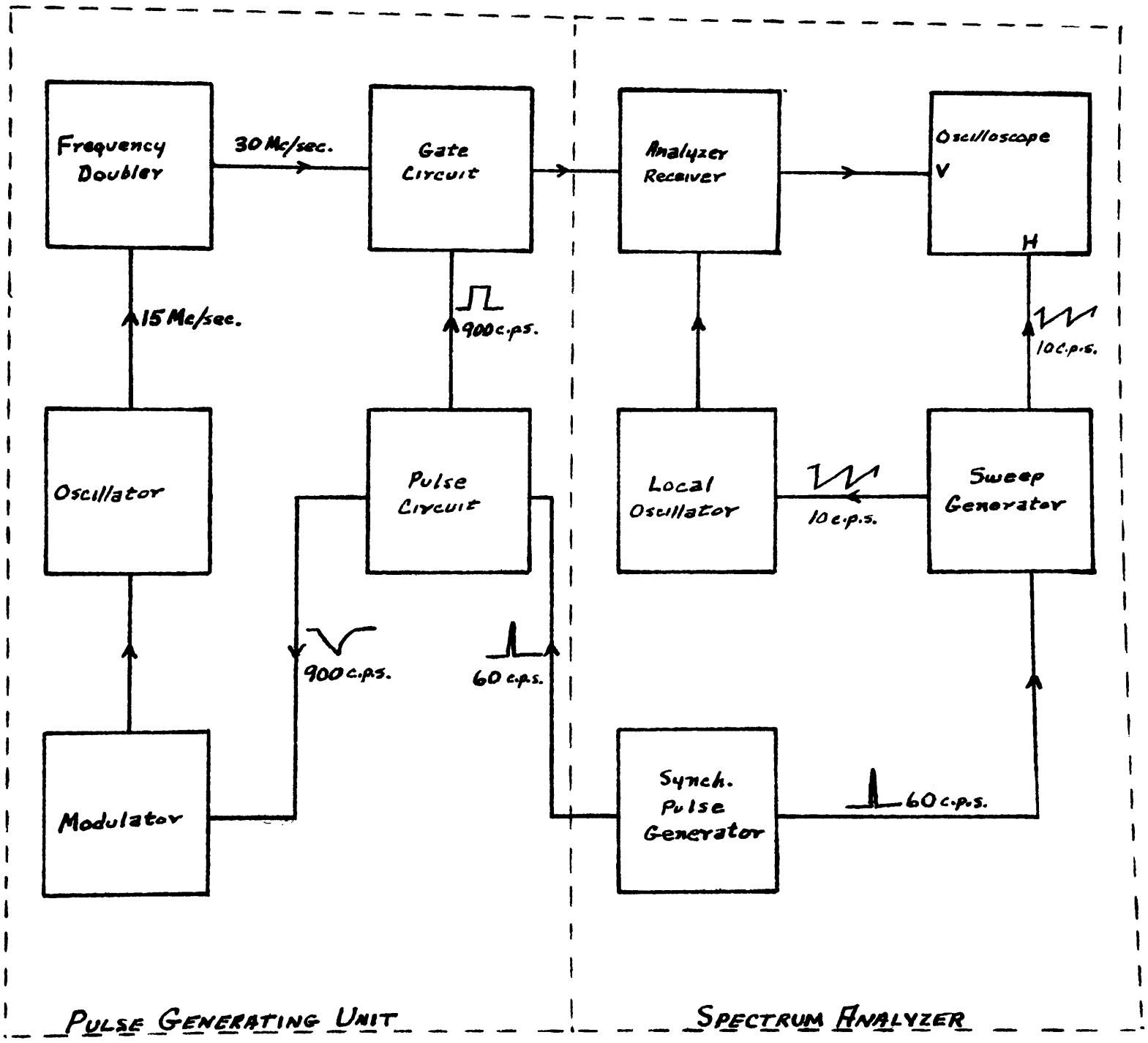

Fig. 3.

Block Diagram of Analogue Computor

3: 2. The Reactance Modulator(6)

The desired phase change across the pulse could be effected by phase modulation, or by frequency modulation, of the oscillator. Of the two methods the use of frequency modulation requires fewer and more easily adjusted components, with very much less amplitude modulation; hence the use of frequency modulation was chosen.

Fig. 4 shows the equivalent circuit of a typical reactance tube modulator connected across an oscillator tank circuit.

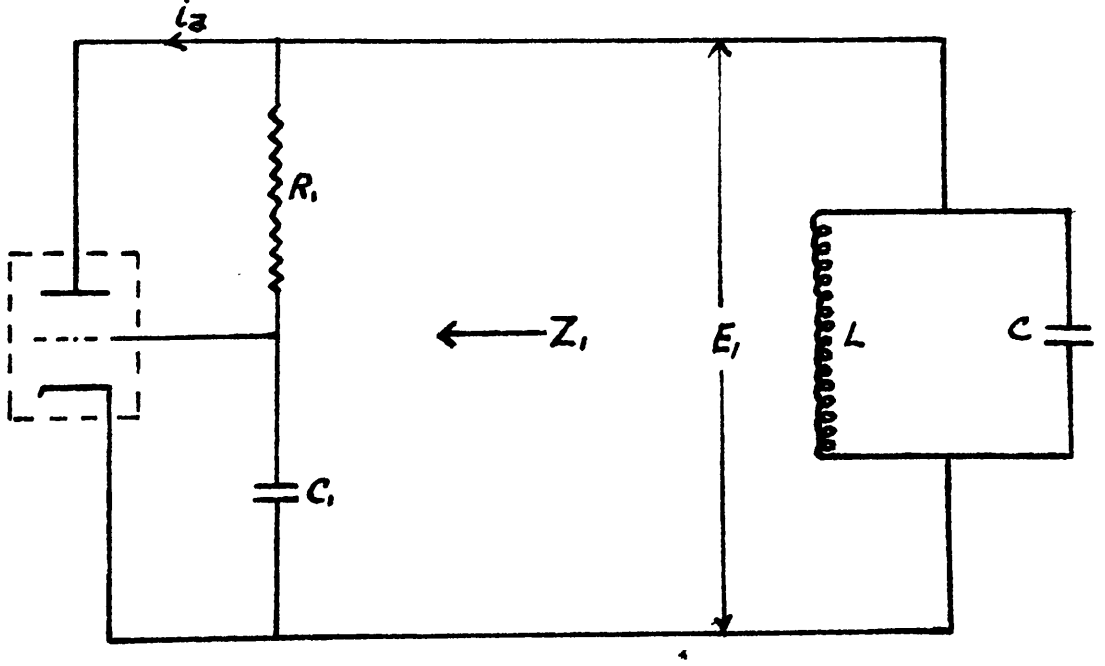

Fig. 4

Equivalent circuit of reactance tube modulator.

$$i_a = G_m e_g + \frac{e_a}{h_p} = G_m \left[\frac{\frac{1}{j\omega C_1}}{R_1 + \frac{1}{j\omega C_1}} \right] E_1 + \frac{E_1}{h_p} = E_1 \left[\frac{1}{h_p} + \frac{G_m}{1 + j\omega R_1 C_1} \right]$$

$$\frac{1}{Z_1} = \frac{1}{R_p} + \frac{G_m}{1+j\omega R_1 C_1} \doteq \frac{G_m}{j\omega R_1 C_1}$$

$$\therefore Z_1 = j\omega \frac{R_1 C_1}{G_m} = j\omega L_1 \qquad (27)$$

The above approximations are valid for a pentode such as the 6AC7, where w = $2\pi \times 15$ Mc/sec., R = 82,000 ohms, C = 10^{-11} farads. Equation (27) indicates that the reactance tube effectively puts an inductance L_1 across the oscillator tank circuit. The total effective inductance L_e is then:

$$L_e = \frac{LL_1}{L+L_1} = \frac{LR_1C_1}{LG_m + R_1C_1}$$

$$\omega^2 = \frac{1}{CL_e} = \frac{G_m}{CR_1C_1} + \frac{1}{LC}$$

$$2\omega \cdot \Delta\omega = \frac{\Delta G_m}{CR_1C_1}$$

$$\therefore \Delta\omega = \Delta G_m \frac{1}{2\omega CR_1C_1} \doteq \Delta G_m \frac{1}{2\omega_0 CR_1C_1} \qquad \{as\ \omega \doteq \omega_0\} \qquad (28)$$

Hence frequency deviation depends linearly on changes in mutual conductance of the reactance tube for $\Delta w \ll w_0$.

The choice of a 6AC7 as a reactance tube was made because it was readily available, and its characteristics for a plate supply voltage of 300 volts showed a mutual conductance characteristic curve linear over a large change in g_m. It was necessary to determine operating conditions at a plate supply voltage of 250 volts.

This was done by plotting changes in oscillator frequency for changes in grid bias of the modulator, with different fixed values of screen grid voltage. A graph of values found satisfactory is shown in Fig. 7.

To represent a phase change of 3.2π across the mouth of a horn, the frequency deviation at 30 Mc/sec. must be 64 Kc/sec.. This means a deviation of 32 Kc/sec. at the oscillator frequency of 15 Mc/sec.. The actual circuit used to obtain the desired modulation was that of V7, Fig. 6. Bias was obtained by means of a by-passed cathode resistor, while the screen grid decoupling condenser maintained that electrode at constant potential. The condenser C, of Fig. 4 was merely the grid-cathode capacity of the tube.

3: 3. <u>The Oscillator and Frequency Doubler</u>

The frequency modulated oscillator (V8,Fig. 6) was constructed to operate at a centre frequency of 15 Mc/sec.. Its output was passed through a broad band frequency doubler, V9, to supply the operating frequency of 30 Mc/sec..

A 6J5 triode was connected as a conventional Hartley oscillator, with the reactance modulator connected across the tank circuit as shown. The frequency doubler was an amplifier with a tuned circuit as its plate load tuned to 30 Mc/sec.. A resistor R35 across this tuned circuit lowered the Q of the circuit and thus made it broad enough to accomodate sidebands introduced by

frequency modulation. The band pass should be at least 1.4 Mc/sec. (Section 2: 3). With the values of L2, R35, and C24 used

$$Q = \frac{\omega_0 C}{G} = 21.7 = \frac{f_0}{2(f_0 - f)}$$

$$\therefore 2(f_0 - f) = \frac{f_0}{21.7} = 1.38 \text{ Mc/sec.} \qquad (29)$$

Thus the output of the frequency doubler at 0.69 Mc/sec. off the centre frequency would be 0.70% of the output at the centre frequency. Actually it should be the same. This could be more nearly approached by stagger-tuning grid and plate tuned circuits, instead of having only a tuned circuit in the plate circuit of the tube; or by stagger-tuning the existing tuned circuits in the plate of V9 and the plate of V10. The latter method was the one employed.

3: 4. The Gating Circuit

The requirements of the gating circuit were that it should only pass the 30 Mc/sec. oscillations, at constant amplitude, for 50 μsec. at a 900 c.p.s. rate. A simple and effective method of accomplishing this was to bias a pentode beyond cut-off and apply a 50 μsec. positive pulse to the control grid at a P.R.F. of 900 c.p.s.. The signal voltage from the doubler stage was also fed to the grid. An attempt was made to apply the signal to the suppressor grid, but it appeared at the plate of the tube even though the tube was cut off, due to the capacity

between electrodes. Even with the connections used, it was found necessary to place a copper shield across the base of the tube, to eliminate direct pick-up between input and output electrodes.

A coaxial line was used between the gate tube and the analyzer, but in the final design of the computor it is suggested that all units be mounted on one chassis or rack for simpler interconnection.

3: 5. The Pulse Generating Circuit

The requirements on the pulse generator were threefold:

(1) To produce a 50 μsec. gating pulse;

(11) To produce a 50 μsec. sawtooth waveform in synchronism with the gating pulse;

(111) To operate at a P.R.F. of 900 c.p.s. in synchronism with the timebase sweep frequency of 10 c.p.s. of the spectrum analyzer.

A type of phantastron[7] was constructed to perform the first two operations simultaneously. The output from the plate is a negative-going linear sawtooth, while a positive square pulse is obtained from the screen grid. The circuit is quiescent until triggered, and then for each trigger pulse applied to the suppressor grid the required waveforms are produced. The diode V5a is used to set the plate voltage so that the suppressor grid bias keeps the plate current cut-off until a positive trigger pulse allows plate current to flow. The plate to grid coupling condenser C12 adjusts pulse width. The waveforms

at the various electrodes of V4 are shown in Fig. 4b.

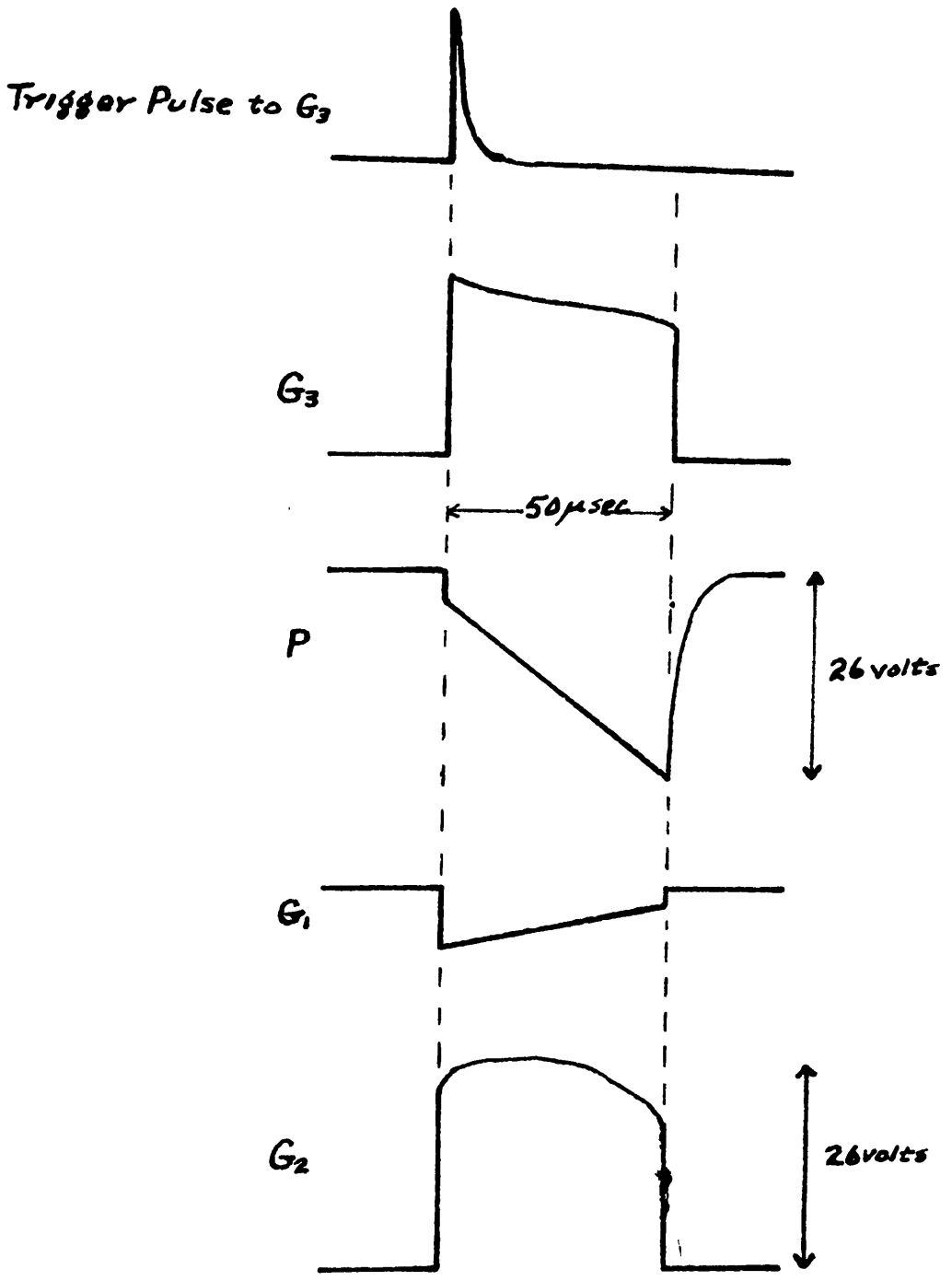

Fig. 4b

The output from the plate of V4 was taken through a blocking condenser C13, potentiometer R19, and resistors R27 and R28 to the grid of V7 as a modulating voltage. The nearly square positive pulse from the screen grid of V4 was amplified and squared by the two stages V6a, V6b, and then applied as a 50 μsec. positive pulse to the gate tube V10.

The 60 c.p.s. supply voltage was amplified, squared, and differentiated to give 60 c.p.s. pips, the operation being performed in a part of the spectrum analyzer circuit. The analyzer sweep circuit divided by 6 to operate at 10 c.p.s., while the 15th harmonic of 900 c.p.s. was selected by a twin-T amplifier V2. It was then amplified and squared in the two stages V3a, V3b, differentiated, and applied to the pulse tube V4 as a trigger pulse at a P.R.F. of 900 c.p.s..

4. Experimental Results

4: 1. The Twin-T Amplifier

The frequency response of the tuned amplifier V2 was studied by applying a continuous signal from an audio oscillator to the grid of V1 and measuring the output of V2 at different frequencies. Adjustment of the variable resistor R9 in the feedback circuit allowed the response to be set to a maximum at 900 c.p.s.. Fig. 5 shows a plot of output vs. frequency for V2, indicating the narrow bandwidth of the amplifier, which ensured passage of only the 15th harmonic of the 60 c.p.s. synchronizing pulse.

With the synchronizing pulse applied to the grid of V1, the output of V2 was a 900 c.p.s. sine wave, which had a maximum amplitude coincident with the synchronizing pulse and fell off to about 80% of that value before the arrival of the next synchronizing pulse. The form of the sine wave appeared to be slightly distorted by the synchronizing pulse, just for one cycle, causing in

effect a slight jitter of the 900 c.p.s. waveform when viewed on an expanded timebase. The amplitude of the synchronizing pulse was reduced to a minimum consistent with positive 900 c.p.s. production, but the jitter, though reduced, persisted. Causing the feedback circuit to oscillate at 900 c.p.s. by itself showed no jitter, but of course the frequency of oscillations was not stable enough to remain in phase with the 60 c.p.s. supply frequency.

The effect of the jitter on the cathode ray tube display was to give pulses varying in amplitude at an uneven rate. The overall pattern was quite stable, however. Because of the pulse jitter, the analyzer would not select the identical frequency component of the spectrum of the pulse at the same position on the timebase sweep. The effect, being small, would not destroy the overall spectrum display, but would only cause the individual pulses of the display to vary rapidly in amplitude by a small amount. This is an undesirable state of affairs which it is believed can be corrected by a method to be discussed under "Conclusions".

4: 2. <u>The Gating Pulse and Modulating Pulse</u>

The positive pulse at the screengrid of V4 had an amplitude of 26 volts, but was not completely square. The width of the pulse was set to 50 µsec. by adjustment of the plate grid coupling condenser C12. Two stages of

amplification brought the pulse out at the plate of V6b as a 100 volt positive pulse with steep sides and a slightly rounded top. As the grid swing of the gate tube was only 24 volts, the pulse from the plate of V6b ensured sharp cut-on and cut-off of the gate tube. A small resistor was placed temporarily in the plate circuit of the gate tube so its output could be observed on an oscilloscope, and the 50 microsecond pulse appearing at the plate of V10 was a true square wave, with a time lag in its edges so slight it could not be detected on a 30 microsecond, 2 inch timebase.

The plate of V4 produced a negative-going linear saw-tooth waveform of 50 μsec. duration and 26 volts amplitude.

4: 3. Modulation Linearity

No equipment was available to accurately measure the shift in oscillator frequency for a given change in modulator bias, as the total frequency shift required was such a small percentage of the centre frequency. An approximate determination of linearity was made as follows: the ungated signal was passed to the spectrum analyzer by removing the bias and gating pulse from V10, and the shift in frequency for given changes in modulator bias observed directly on the analyzer cathode ray tube, with the time base duration representing 200 Kc/sec.. As the modulator bias was changed, the signal moved to a new position on the

time base. A graph of the results is shown in Fig. 7.

4: 4. Circuit Stability

The only part of the equipment sensitive to parts replacements is the twin-T feedback circuit comprised of resistors R3, R4, R7, R8, and condensers C2, C5, C6 and C7. All other components have a tolerance of 20% without affecting proper operation. None of the tubes operate at critical positions on their characteristic curves, so they may be replaced without upsetting stability.

4: 5. Displays(8)

Display 1, Fig. 9, shows a photograph of the pattern representing a radiating horn with a/λ ratio of 15, and plane illumination of the aperture. For signals from the analyzer receiver well below saturation level, the gain characteristic of the receiver was quite linear; but near saturation it became very non-linear. Hence the amplitude of the central lobe with respect to the side lobes is not a true representation. Actual measurements of the amplitudes of the side lobes were made and compared with the theoretical values, and the comparison is very good. In Table 2 below "Max." indicates the maximum numbered from the centre as 1, 2, etc., "g" indicates the theoretical amplitude with respect to that of the central maximum being 1.00 and "G" shows the amplitude measurement made on the photograph, in inches.

Table 2

Max.	1	2	3	4	5
g	0.217	0.128	0.091	0.071	0.058
G	2.19	1.52	1.00	0.74	0.52

Fig. 8 shows how the analyzer receiver began to saturate for large signal input, which accounts for the discrepancy in the relative amplitudes of the lobes in the display.

The positions of the maxima and minima with respect to sin θ agree with the theoretically calculated values within the errors of measurement on the photograph. Table 3 shows these comparisons.

Table 3

Min. No.	Measured sin θ	Calculated sin θ	Max. No.	Measured sin θ	Calculated sin θ
1	0.06	0.066	0	0	0
2	0.14	0.133	1	0.09	0.094
3	0.20	0.200	2	0.18	0.165
4	0.27	0.267	3	0.23	0.232
5	0.34	0.333	4	0.31	0.298
6	0.41	0.400	5	0.36	0.365
7	0.46	0.466	6	0.42	
8	0.52	0.533	7	0.50	
9	0.60	0.600	8	0.56	
10	0.65	0.667	9	0.62	

The tables used in calculating sin θ for the positions of the maxima did not carry beyond the fifth maximum.

Display 2, Fig. 10, shows the pattern for $a/\lambda = 15$, and a phase change across the mouth of the horn of 1.5π . Multiplying equation (12) by $e^{-j\frac{3\pi}{2}}$ gives (12a) multiplied by j, showing a shift of 90° or $\frac{\pi}{2}$ in the positions of the maxima and minima of the radiation pattern. The photograph shows that such is the case, as at sin θ = 0 a minimum now appears, and at sin θ = 0.06, etc. appear maxima. Compare the values of sin θ for the minima and maxima in Table 4 with the values of sin θ for the maxima and minima respectively in Table 3.

Table 4

Min. No.	Measured sin θ	Max. No.	Measured sin θ
0	0	1	0.06
1	0.13	2	0.15
2	0.21	3	0.23
3	0.27	4	0.29
4	0.32	5	0.35
5	0.40	6	0.41
6	0.45	7	0.48
7	0.51	8	0.53
8	0.58	9	0.60
9	0.63	10	0.67

The dissymmetry in the display pattern is the result of several factors, the main one being the tuning of tank circuits in both the pulse generating unit and the spectrum analyzer. The experimental layout was not conducive to rapid and accurate alignement.

Display 3, Fig. 11, shows the pattern for $a/\lambda = 12$, plane illumination of the aperture. Table 5 gives the measured and calculated values of sin θ for the positions of the minima and maxima, again indicating good correspondence. Amplitude dissymmetry is again quite evident.

Table 5

Min. No.	Measured sin θ	Calculated sin θ	Max. No.	Measured sin θ	Calculated sin θ
1	0.08	0.083	1	0.12	0.118
2	0.16	0.166	2	0.20	0.205
3	0.24	0.250	3	0.28	0.288
4	0.34	0.333	4	0.36	0.372
5	0.43	0.417	5	0.45	0.455
6	0.52	0.500	6	0.54	
7	0.56	0.582	7	0.60	
8	0.65	0.667			

Display 4, Fig. 12, is the pattern for $a/\lambda = 3$, plane illumination of the aperture. Table 6 gives the values of sin θ for the first two minima, and for the first secondary maximum.

Table 6

Min. No.	Measured sin θ	Calculated sin θ	Max. No.	Measured sin θ	Calculated sin θ
1	0.36	0.333	1	0.52	0.47
2	0.66	0.667			

The uneven portrayal of the patterns with respect to the two side lobes of the centre of the pattern is due mainly to the non-linear frequency sweep of the oscillator of the spectrum analyzer. Display 4, Fig. 13, is a photograph of frequencymarkers on the timebase at intervals of 100 kilocycles per second. It can be seen that the right hand end of the sweep is expanded more; this effect is most apparent in the display of Fig. 12. The left half of the sweep is fairly linear, and all the measurements of sin θ values for all patterns shown were made on that side of the central lobe.

5. Conclusions and Recommendations

The frequency modulated pulse unit as a whole operated satisfactorily except for some synchronization difficulties. Initially a multivibrator operating at 900 c.p.s. was used as the master control, where it performed the operations of triggering the pulse-producing tube V4 as well as synchronizing the analyzer time base sweep generator. The latter was done by dividing the 900 c.p.s. frequency down to 60 c.p.s. and using that as a

synchronizing pulse; however, as it did not remain in phase with the 60 c.p.s. supply, interference from the latter caused instability. It is suspected that this interference was the result of poorly regulated power supplies, and insufficient or no shielding of leads. With the computor built as one complete unit, with a common well-regulated power supply, there is no apparent reason why the system would not be entirely satisfactory.

That the jitter in the gating pulse was responsible for the instability of the display was shown as follows: the 60 c.p.s. synchronizing pulse was removed from V1, and the output of an audio oscillator was injected at the grid of V3b. Its frequency was adjusted to 240 c.p.s., giving a gate pulse at a P.R.F. of 240 c.p.s.. The resulting display pulses were 24 in number instead of 90, with the expected separation between them. If the audio oscillator frequency could be held at exactly 240 c.p.s., the display pulses remained stationary in amplitude and position, and examination of the gating pulse on the expanded time base of an auxiliary oscilloscope indicated no jitter whatever. As the frequency drifted off 240 c.p.s., the display pulses moved along the timebase, and their amplitude varied as the envelope of the frequency spectrum of the gating pulse. Hence if the gating pulse, though occurring at a constant 900 c.p.s., should jitter, the part of its spectrum displayed at a given position on the

time base would vary as the pulse jitter, resulting in amplitude changes on the display.

The section of the circuit comprised of V1, V2, and V3 should be regarded as a substitute for something better, to be replaced by a master-control circuit such as the 900 c.p.s. multivibrator already mentioned when circumstances warrant the change. The advantages of such a master-control include the possibilities of operating the equipment from a direct current source, or from supplies of frequencies other than 60 c.p.s. such as the 25 c.p.s. supply in parts of Ontario and the 50 c.p.s. supply in Great Britain.

Another consideration to be kept in view is that the computor may be required to give the analogue of antennae with amplitude distributions other than constant, and phase changes across the antennae apertures other than parabolic. Gating pulses and modulating pulses to suit the special conditions in question would have to be developed.

V2 Frequency Response

(Input Amplitude Constant)

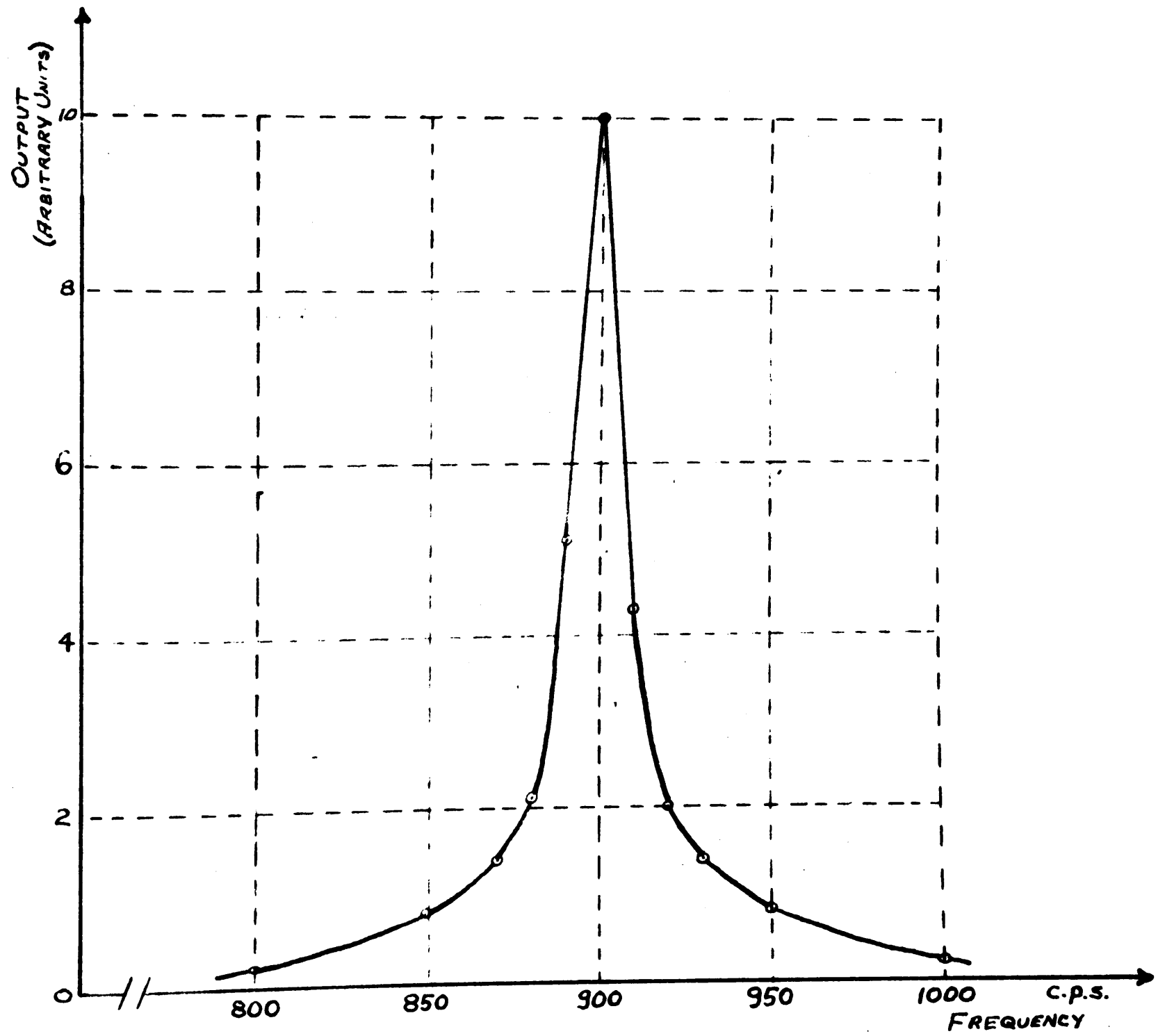

Fig. 5.

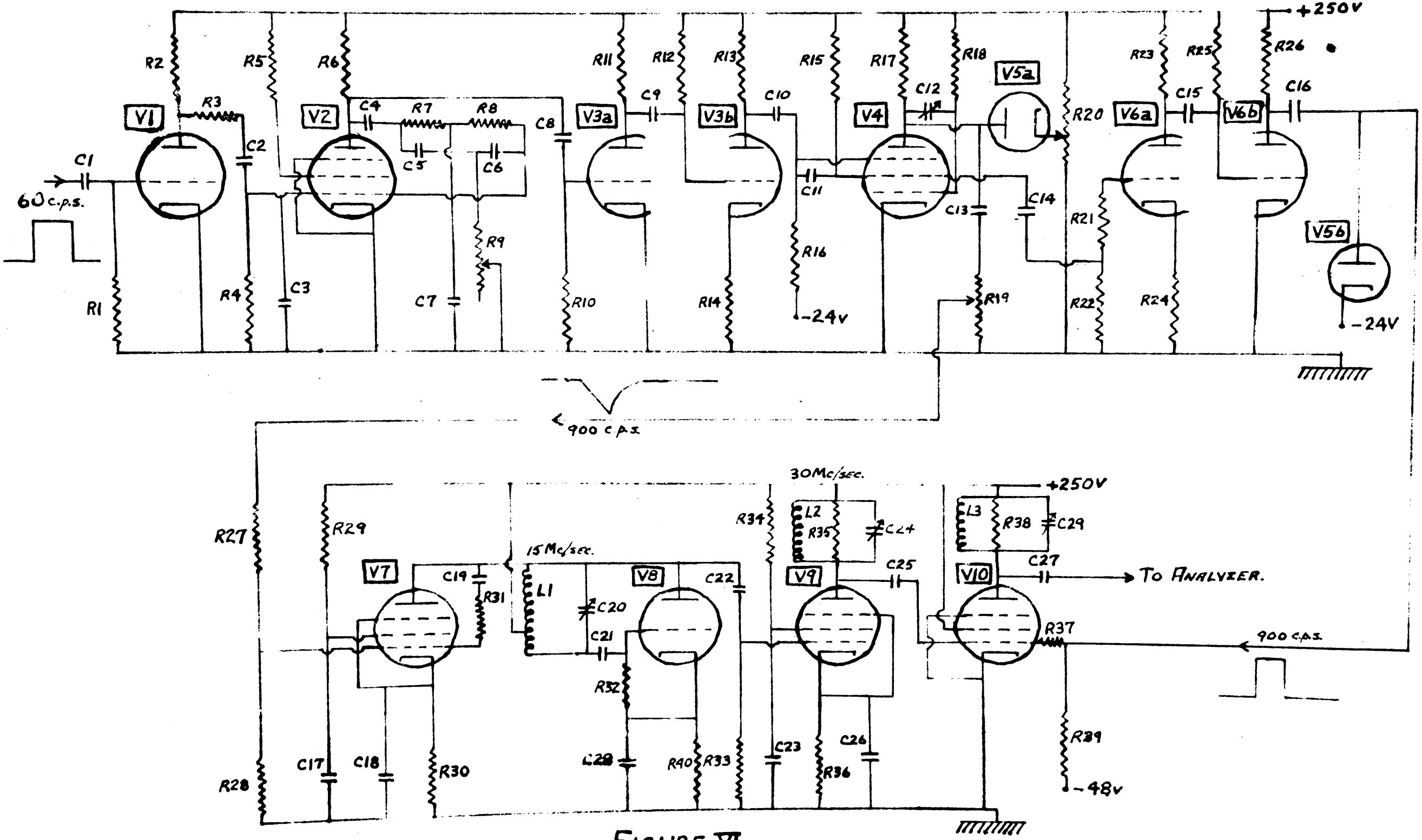

FIGURE VI

CIRCUIT DIAGRAM.

FIGURE VII

MODULATOR OPERATION : 6AC7

E_p = 250 v
E_{c2} = 125 v
E_{c3} = 0 v

OSCILLATOR FREQUENCY : 15 MC/SEC.

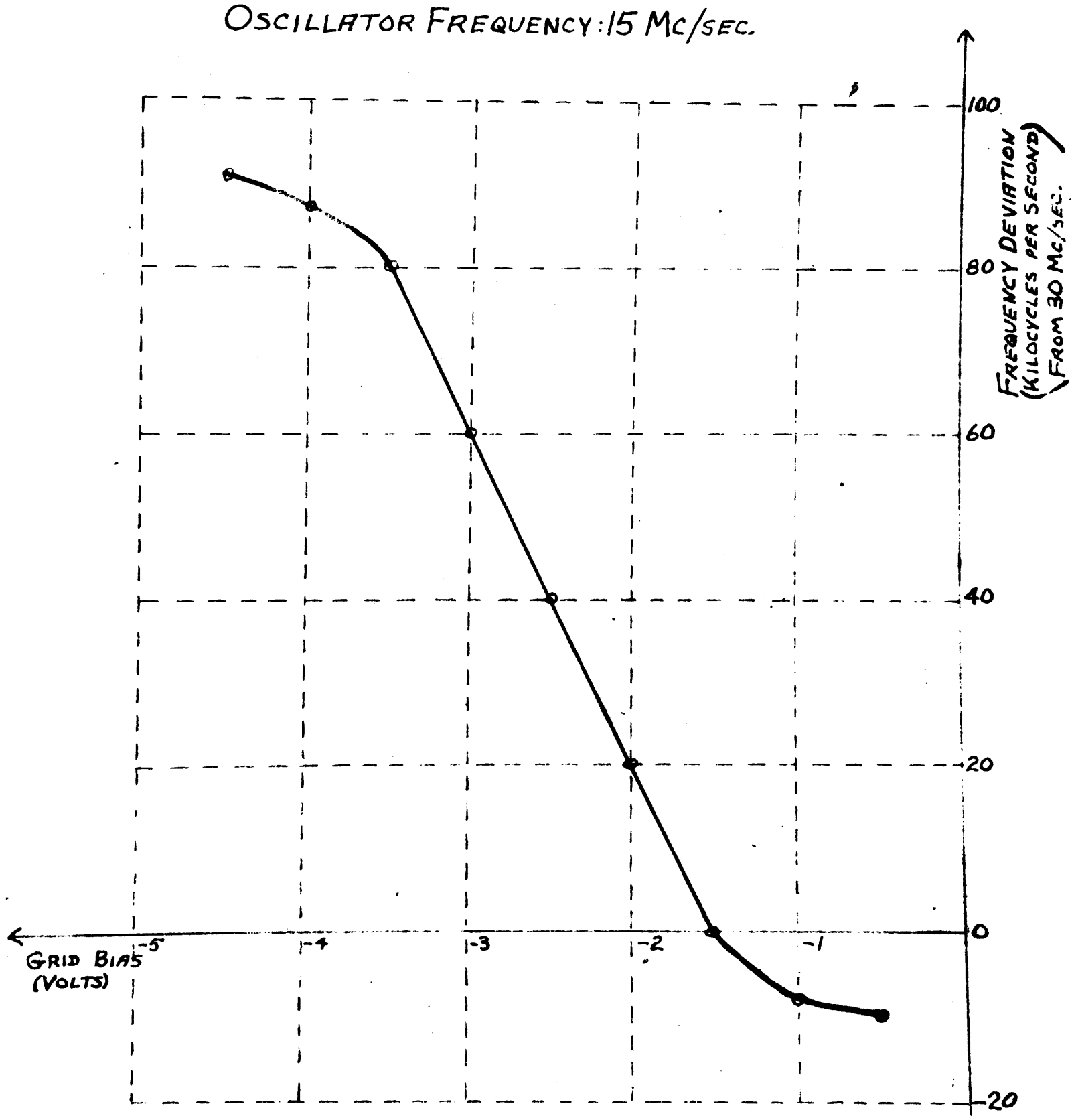

Analyzer Reciever Gain Characteristics.

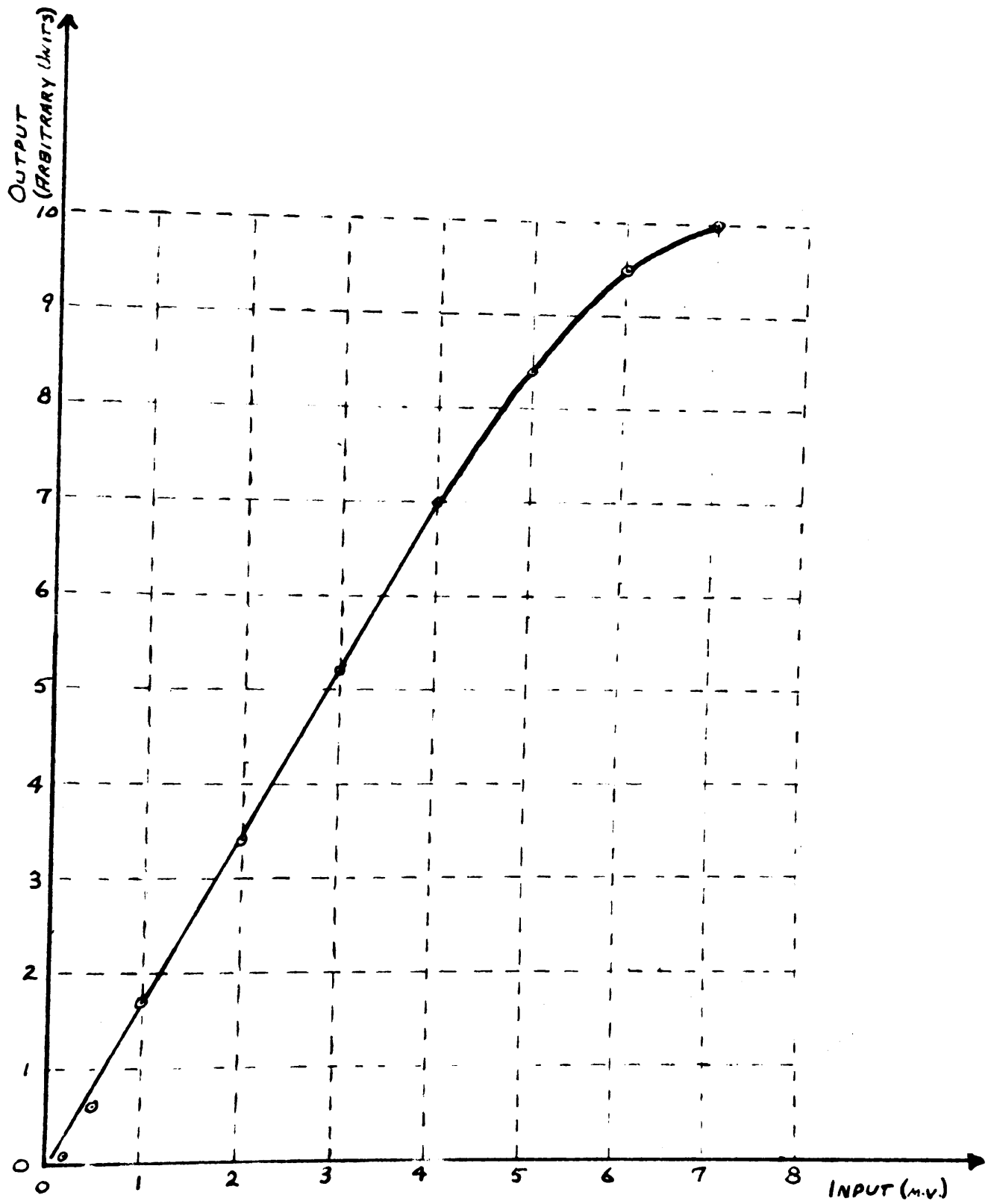

Fig. 8.

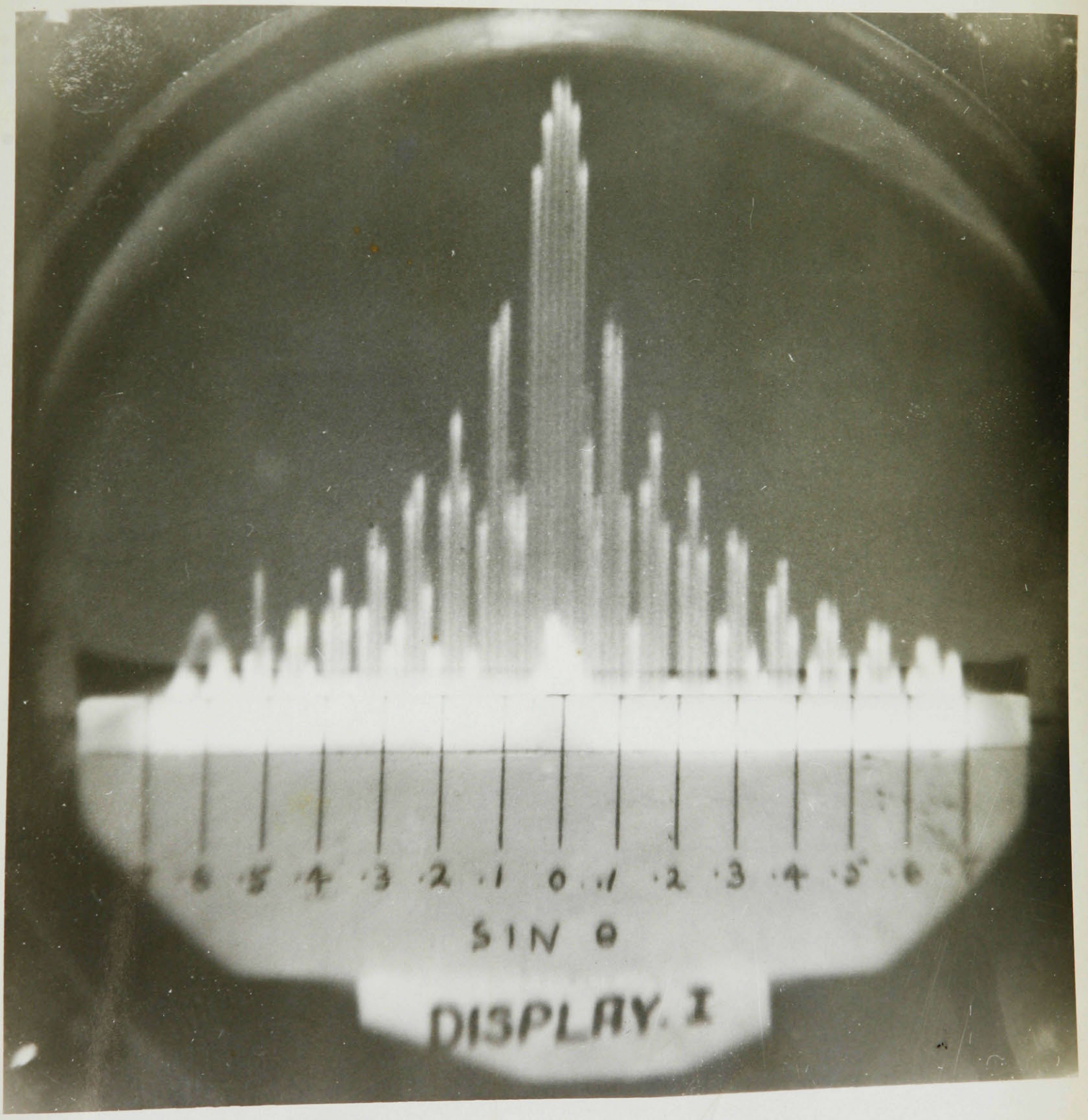

FIG. 9

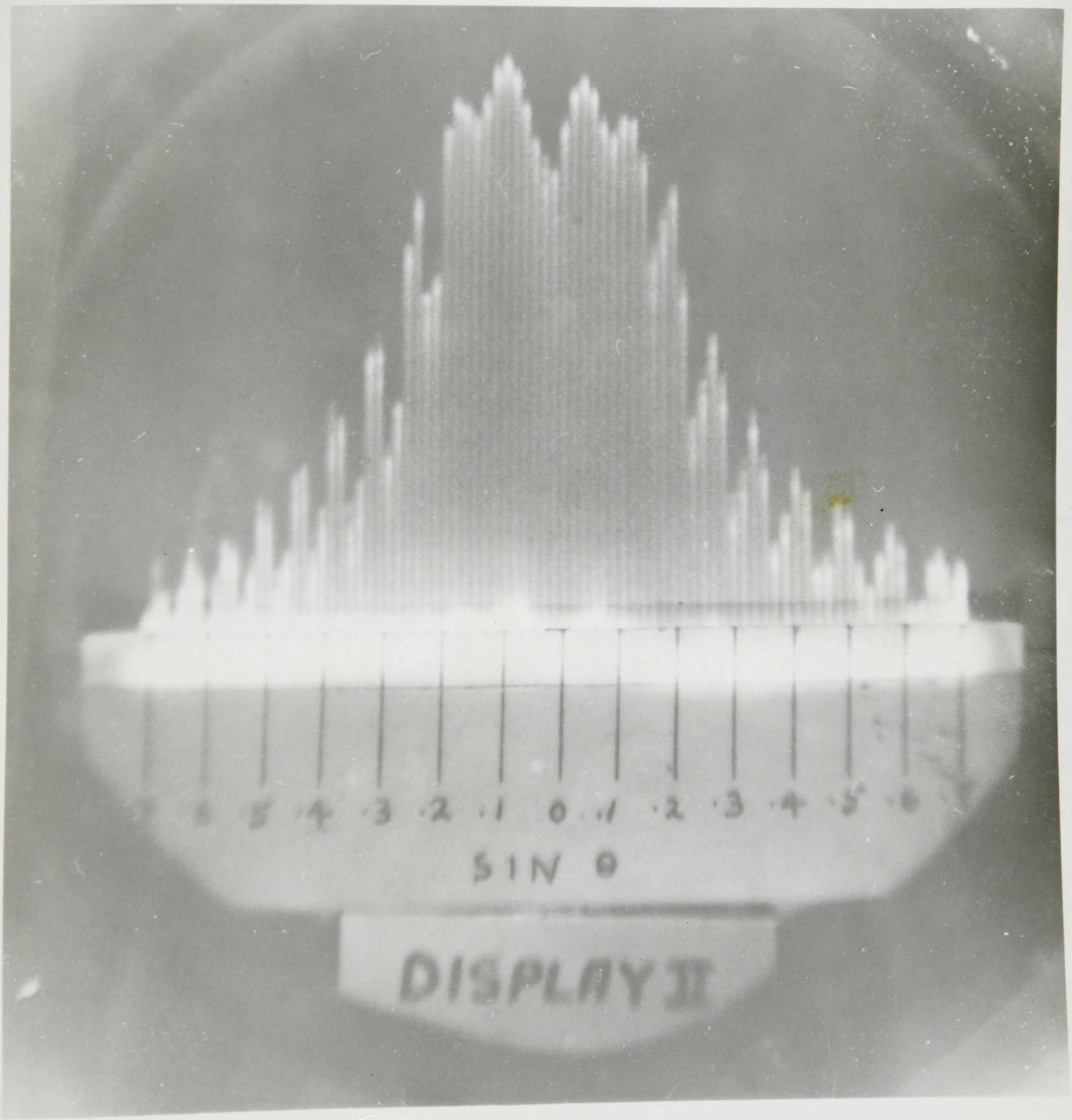

FIG. 10

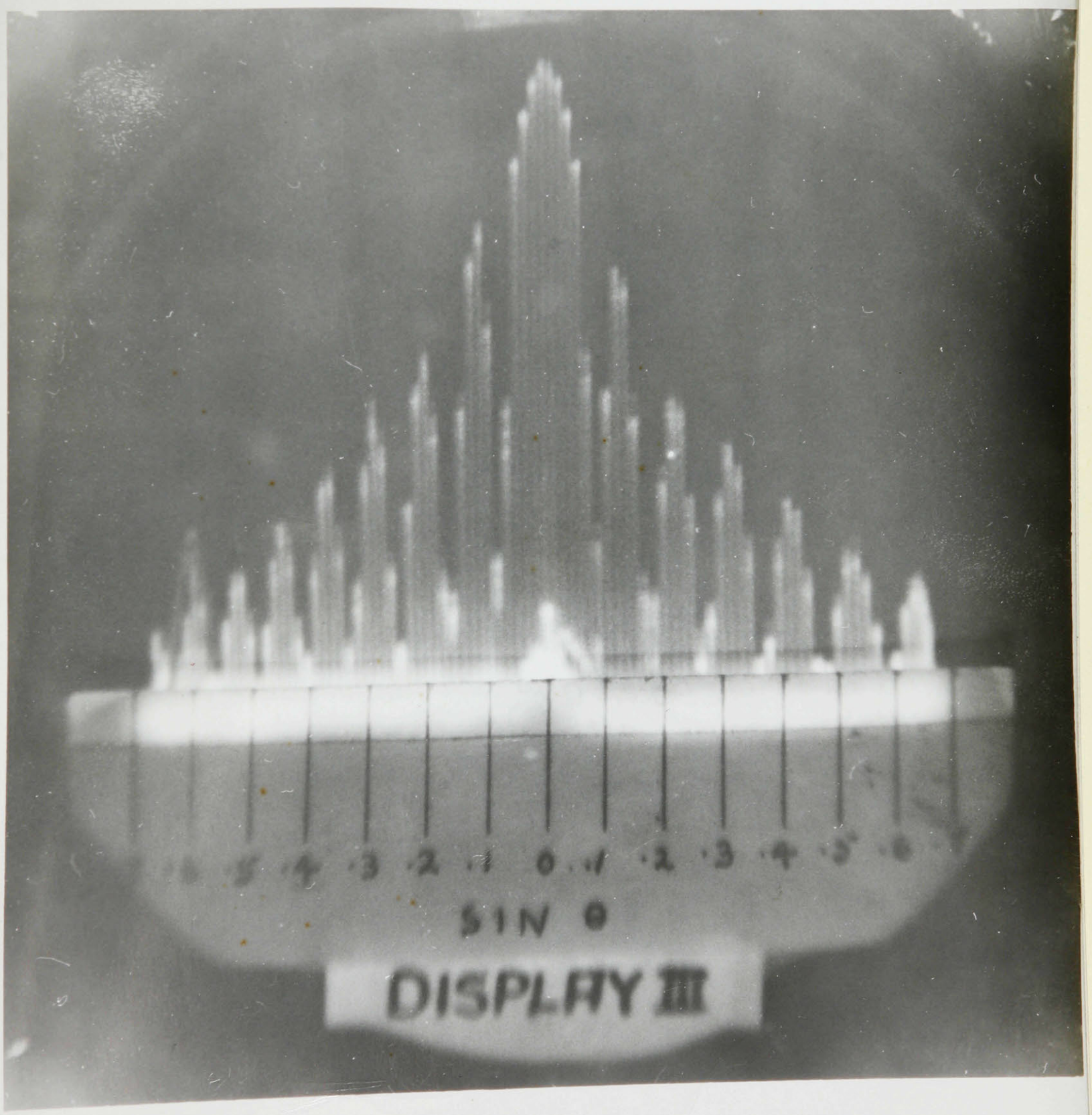

FIG. 11

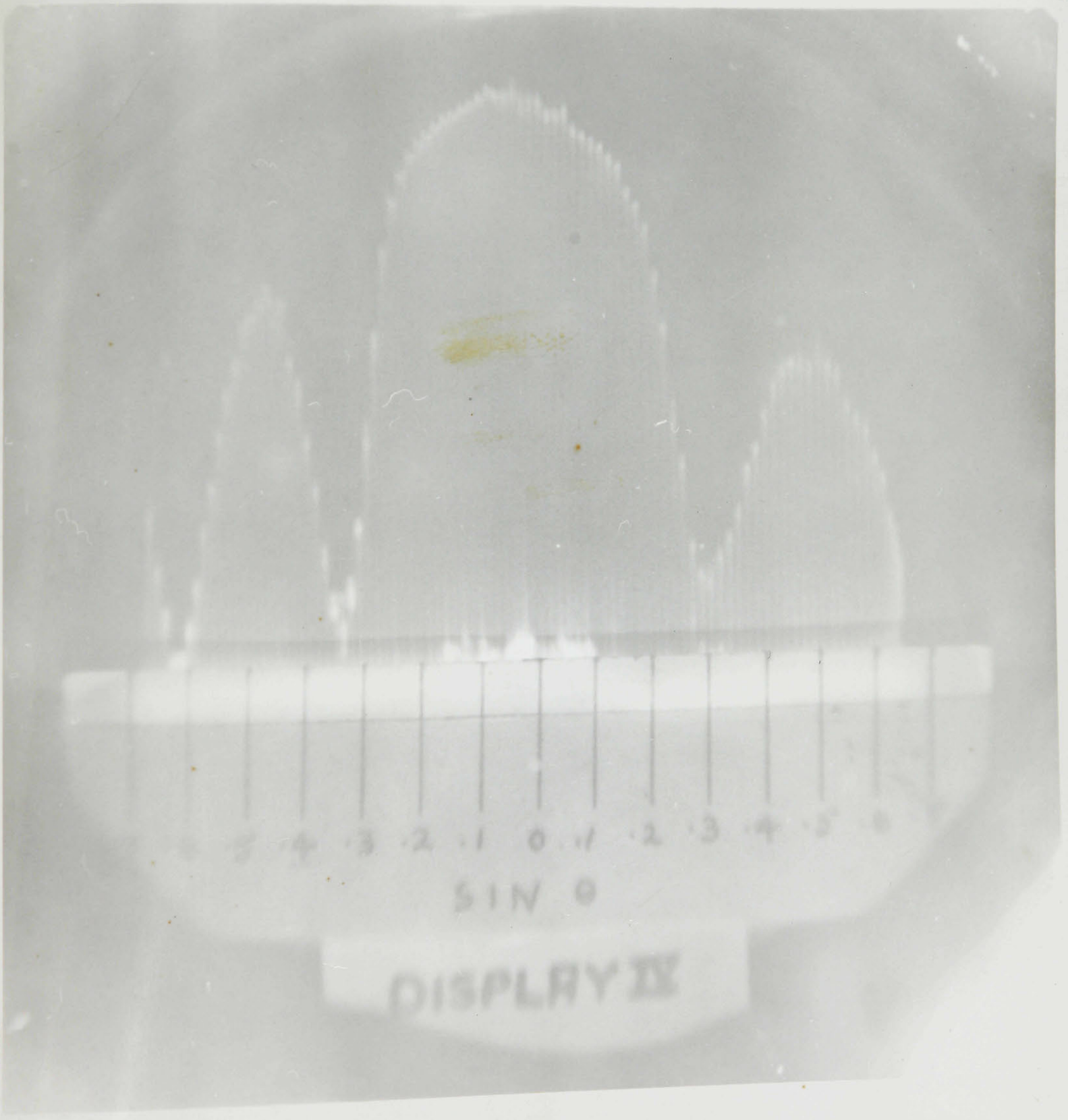

FIG. 12

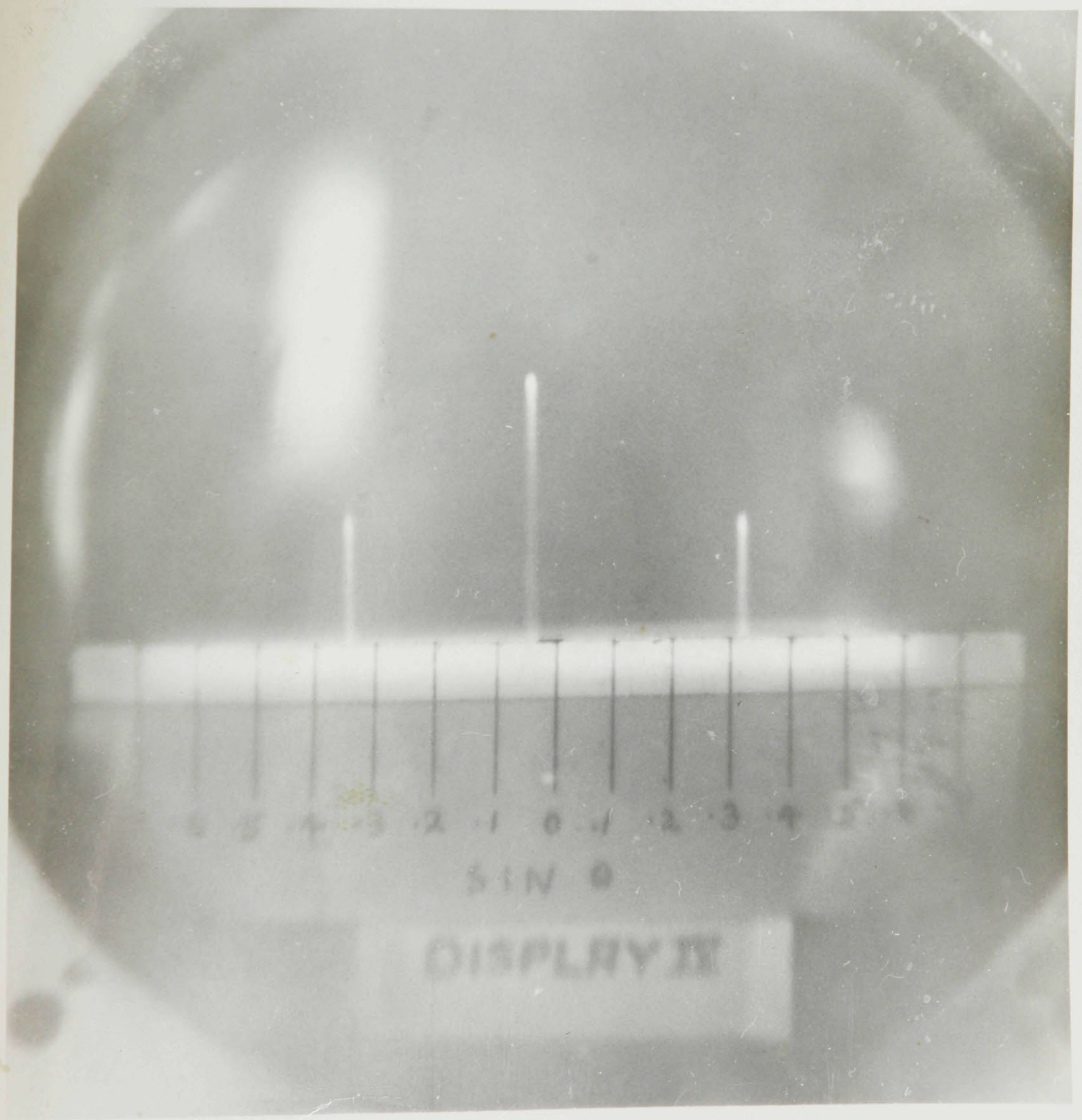

FIG. 13

Table 7

Components parts list

ITEM	DESCRIPTION		
C1	Condenser:	mica: 10$\mu\mu$f	
C2	Condenser:	mica: 300$\mu\mu$f	±5%
C3	Condenser:	paper: 0.01μf	
C4	Condenser:	paper: 0.01μf	
C5	Condenser:	mica: 0.001μf	±5%
C6	Condenser:	mica: 0.001μf	±5%
C7	Condenser:	mica: 0.002μf	±5%
C8	Condenser:	paper: 0.05μf	
C9	Condenser:	mica: 0.001μf	
C10	Condenser:	mica: 10$\mu\mu$f	
C11	Condenser:	mica: 250$\mu\mu$f	
C12	Condenser:	variable: 100-150$\mu\mu$f	
C13	Condenser:	paper: 0.01μf	
C14	Condenser:	paper: 0.005μf	
C15	Condenser:	paper: 0.01μf	
C16	Condenser:	paper: 0.01μf	
C17	Condenser:	paper: 0.01μf	
C18	Condenser:	paper: 0.01μf	
C19	Condenser:	mica: 50$\mu\mu$f	
C20	Condenser:	variable: 3-30$\mu\mu$f	
C21	Condenser:	mica: 100$\mu\mu$f	
C22	Condenser:	mica: 50$\mu\mu$f	
C23	Condenser:	paper: 0.01μf	
C24	Condenser:	variable: 3-30$\mu\mu$f	

Table 7 (cont'd)

ITEM	DESCRIPTION	
C25	Condenser: mica: 25$\mu\mu f$	
C26	Condenser: paper: 0.01μf	
C27	Condenser: mica: 50$\mu\mu f$	
C28	Condenser: paper: 0.001μf	
C29	Condenser: variable: 5-50$\mu\mu f$	
L1	Coil: 4.2μh	
L2	Coil: 2.5μh	
L3	Coil: 2.5μh	
R1	Resistor: 470,000 ohms, $\frac{1}{2}$ watt.	
R2	Resistor: 10,000 ohms, 2 watt.	
R3	Resistor: 1,000,000 ohms, $\frac{1}{2}$ watt.	±5%
R4	Resistor: 1,000,000 ohms, $\frac{1}{2}$ watt.	±5%
R5	Resistor: 470,000 ohms, $\frac{1}{2}$ watt.	
R6	Resistor: 100,000 ohms, 1 watt.	
R7	Resistor: 180,000 ohms, $\frac{1}{2}$ watt.	±5%
R8	Resistor: 180,000 ohms, $\frac{1}{2}$ watt.	±5%
R9	Potentiometer: 500,000 ohms.	
R10	Resistor: 470,000 ohms, $\frac{1}{2}$ watt.	
R11	Resistor: 82,000 ohms, $\frac{1}{2}$ watt.	
R12	Resistor: 470,000 ohms, $\frac{1}{2}$ watt.	
R13	Resistor: 82,000 ohms, $\frac{1}{2}$ watt.	
R14	Resistor: 2,000 ohms, $\frac{1}{2}$ watt.	
R15	Resistor: 100,000 ohms, $\frac{1}{2}$ watt.	
R16	Resistor: 100,000 ohms, $\frac{1}{2}$ watt.	
R17	Resistor: 100,000 ohms, 1 watt.	
R18	Resistor: 1,000,000 ohms, $\frac{1}{2}$ watt.	

Table 7 (cont'd)

ITEM	DESCRIPTION
R19	Potentiometer: 1,000,000 ohms.
R20	Potentiometer: 100,000 ohms.
R21	Resistor: 100,000 ohms, ½ watt.
R22	Resistor: 500,000 ohms, ½ watt.
R23	Resistor: 100,000 ohms, ½ watt.
R24	Resistor: 1,200 ohms, ½ watt.
R25	Resistor: 220,000 ohms, ½ watt.
R26	Resistor: 10,000 ohms, 2 watt.
R27	Resistor: 270,000 ohms, ½ watt.
R28	Resistor: 22,000 ohms, ½ watt.
R29	Resistor: 100,000 ohms, ½ watt.
R30	Resistor: 470 ohms, ½ watt.
R31	Resistor: 82,000 ohms, ½ watt.
R32	Resistor: 47,000 ohms, 1 watt.
R33	Resistor: 220,000 ohms, ½ watt.
R34	Resistor: 100,000 ohms, ½ watt.
R35	Resistor: 10,000 ohms, ½ watt.
R36	Resistor: 390 ohms, ½ watt.
R37	Resistor: 100,000 ohms, ½ watt.
R38	Resistor: 3,300 ohms, 2 watt.
R39	Resistor: 1,000,000 ohms, ½ watt.
R40	Resistor: 39,000 ohms, 2 watt.
V1, V8	Vacuum tube: 6J5
V2, V4	Vacuum tube: 6SJ7
V3, V6	Vacuum tube: 6SN7
V5	Vacuum tube: 6H6
V7, V9, V10	Vacuum tube: 6AC7

BIBLIOGRAPHY

(1) Slater and Frank: "Electromagnetism": Eqn. (2.2) p. 171

(2) Slater and Frank: "Electromagnetism": Eqn. (2.3) p. 172

(3) Ramsay: "Fourier Transforms in Aerial Theory": The Marconi Review, Vols. 9,10,11, Oct.-Dec. (1946)

(4) Otto Schmidt: J.A.P. 18, p.819, Sept. (1947)

Carl Berkley: P.I.R.E. 36, p.1530 (1948)

(5) G.A. Woonton: "Theoretical and Practical Considerations of the Design of a Diffraction Field Computor": McGill University, Physics Dep't., Aug. 28, 1949 (unpublished).

(6) A. Hund: "Frequency Modulation": p. 166

(7) M.I.T. Radiation Laboratory Series, Vol. 19, p. 197

(8) M.I.T. Radiation Laboratory Report S-8: "Tables of Fourier Transforms of Fourier Series, Power Series and Polynomials".

Appendix

Alignment Procedure

(1) Connect an audio oscillator to the grid of V1 in place of the 60 c.p.s. synchronizing pulse. Adjust its frequency to 900 c.p.s.. With an oscilloscope whose time base is locked to 60 c.p.s. and has 60 sweeps per second, observe the output of V2 at the grid of V3a. Adjust the potentiometer R9 for maximum response, which should also give 15 stationary cycles on the time base. Disconnect the oscillator and reconnect the synchronizing pulse lead to the grid of V1. A finer adjustment of R9 will improve the regularity of the 900 c.p.s. sine wave observed on the oscilloscope.

(2) Connect the oscilloscope to the plate of V5b, which will give an observation of the gating pulse. Bring the cathode of V5a from ground potential by means of the potentiometer R20. As the plate of V4 rises in voltage, spurious pulses will appear first, then 15 stable pulses, then suddenly a great many more than 15 pulses. Leave R20 set just below the last mentioned condition, so that there are 15 stable pulses on the time base. Switch the oscilloscope time base sweep to a known duration in the neighbourhood of 100 μsec.. Observe the gate pulse, and adjust C12 until the width of the pulse is 50 μsec..

(3) Turn the centre-tap of R19 to ground. Connect an oscillator to the grid of V10, tuned to 30 Mc/sec..

Adjust the preset condenser C29 to give a maximum signal on the spectrum analyzer oscilloscope trace. Move the oscillator output to the grid of V9 and similarly adjust C24. By alternately adjusting C24 and C29 and sweeping the oscillator about 30 Mc/sec. so the signal moves over the oscilloscope trace, a condition may be attained where the signal maintains a constant amplitude as it moves from one end of the trace to the other. This means that the tuned circuit at the plate of V9 will be tuned slightly on one side of 30 Mc/sec., and the tuned circuit at the plate of V10 slightly on the other side. Remove the external oscillator from the grid of V9. Adjust condenser C20 to give a signal centered on the spectrum analyzer oscilloscope trace.

(4) The pattern appearing on the cathode ray tube will be a diffraction pattern of a certain type, depending on the frequency sweep representation of $2(f_o-f)$. As the centre tap of potentiometer R19 is moved away from ground potential, the shape of the pattern will change. By measuring the amplitude of the modulating waveform at the tap of R19 by means of an auxiliary oscilloscope, the amplitude of the waveform appearing at the grid of V7 can be computed by means of the ratio of R28 to R27. Consulting the graph of Fig. 7 will give the amount of frequency deviation obtained for certain voltage changes at the grid of the modulator V7.

By means of the relation given in equation (26)

$$\Delta f = \frac{5a^2}{\lambda \ell} \text{ kc/sec.} \qquad (26)$$

the proper setting of R19 may be obtained to give a pattern representing the distant field from a horn of length "ℓ" cm., width "a" cm., transmitting a frequency of wavelength λ.

Table 8

Significant Voltages

TUBE	ELECTRODE	D.C. VOLTS	A.C. VOLTS
V1	Plate	110	
V2	Plate	95	
	Screen grid	38	
V4	Plate	70	26 (peak) 900 c.p.s.
	Screen grid	40	26 (peak) 900 c.p.s.
	Suppressor grid	-24	
V6b	Plate	88	100 (peak) 900 c.p.s.
V7	Plate	250	
	Screen grid	125	
	Suppressor grid	0	
	Cathode	1.7	
V8	Plate	250	15 Mc/sec.
	Cathode	150	
V9	Plate	250	30 Mc/sec.
	Screen grid	130	
V10	Plate	250	Pulses of 30 Mc/sec. at 900 c.p.s. R.F. Amplitude: 9.4 Volts R.M.S.
	Screen grid	250	
	Control grid	-48	